Aerosol and Air Quality Research, 17: 653–665, 2017

ISSN: 1680-8584 print / 2071-1409 online
doi: 10.4209/aaqr.2016.08.0355

Transformations of Aerosol Particles from an Outdoor to Indoor Environment

Nicholas Talbot[1,2], Lucie Kubelová[1,2], Otakar Makeš[1,2], Jakub Ondráček[1], Michael Cusack[1], Jaroslav Schwarz[1], Petr Vodička[1], Naděžda Zíková[1], Vladimír Ždímal[1*]

[1] *Institute of Chemical Process Fundamentals of the CAS, v.v.i., Rozvojová 2, Prague 165 02, Czech Republic*
[2] *Charles University, Faculty of Science, Department of Environmental Studies, Prague, 128 43, Czech Republic*

ABSTRACT

Aerosol particle size and chemical composition during summer and winter were investigated in this study. An automated switching valve allowed for indoor and outdoor environments to be sampled near-simultaneously with the same high temporal-resolution instrumentation. During the study, no known indoor sources were present and the sampled room was unoccupied throughout.

Accumulation mode indoor/outdoor (I/O) ratios were substantially lower in winter than in summer. This reduction was attributed to particles of outdoor origin shrinking as they entered the warmer and drier indoor environment. An essential factor in this process appeared to be the difference (gradient) between the temperature and relative humidity of the indoor and outdoor environments during the winter. Online aerosol mass spectrometer measurements recorded a 34–38% decrease in I/O ratios for all nonrefractory species during the winter relative to the summer. A similar change in I/O ratios for all species indicated that physical, rather than chemical, processes were responsible.

To assess the relative influence of various physical factors on I/O relationships, Spearman rank statistical tests were carried out. These identified wind speed to be negatively correlated to the indoor concentrations for all species. Wind roses incorporating I/O ratios were applied and showed that the wind speed and direction influenced the changes in the indoor composition. The relative outdoor concentration of different aerosol species, steepness of the I/O temperature gradient, and wind speed variability are concluded to be essential factors in I/O aerosol transformations.

***Keywords*:** I/O ratio; Shrinkage; Dissociation; Aerosols; Ammonium nitrate.

INTRODUCTION

Studies have estimated that people typically spend over 80% of their average day indoors (Lazaridis and Aleksandropoulou, 2008; Leung and Drakaki, 2015). Therefore, a considerable percentage of daily exposure to aerosol particles likely occurs while in confined microenvironments (Long *et al.*, 2001; Hussein *et al.*, 2006; Perez-Padilla *et al.*, 2010). Exposure to aerosol particles has been statistically correlated to numerous serious health consequences, such as respiratory and pulmonary disorders (Pope and Dockery, 2006). Moreover, the indoor migration of outdoor-originating aerosol species has been found to accelerate the degeneration of antiquities in places such as archives and museums (Andelova *et al.*, 2010; Smolík *et al.*, 2013). These epidemiological and environmental concerns render outdoor-to-indoor particle behaviour a key concern in aerosol science.

Indoor aerosol size and composition largely depend on the in-situ emission source, such as cooking, cleaning, or heating (Wallace, 1996; Hussein *et al.*, 2006; Colbeck *et al.*, 2010; Hsu *et al.*, 2012). However, when indoor sources are absent, indoor aerosol concentrations correlate strongly to those outdoors (Lazaridis *et al.*, 2006). This relationship has been detailed in prominent studies worldwide, including those conducted in Athens (Diapouli *et al.*, 2011), Los Angeles (Zhu *et al.*, 2005), Brisbane (Morawska *et al.*, 2001; Guo *et al.*, 2008), Helsinki (Hussein *et al.*, 2004), and Beijing (Han *et al.*, 2016).

In the absence of mechanical ventilation, the influx of outdoor-originating particles is driven by the air exchange rate of a building or room (Chen and Zhao, 2011; Leung and Drakaki, 2015), with the exchange rate dependent on the use, age, and design of the structure (Hering *et al.*, 2007; Levy *et al.*, 2010; Han *et al.*, 2016). Moreover, outdoor aerosol composition affects indoor particle concentration and composition (Brauer *et al.*, 1991; Vette *et al.*, 2001; Morawska *et al.*, 2003; Hussein *et al.*, 2006) with stable compounds such as elemental carbon and SO_4^{2-} favoured over semivolatile polycylic aromatic hydrocarbons and NO_3^-

* Corresponding author.
Tel.: +420220390246
E-mail address: zdimal@icpf.cas.cz

(Huang *et al.*, 2007; Lunden *et al.*, 2008; Poulain *et al.*, 2011; Zhu *et al.*, 2012; Han *et al.*, 2016). In addition, seasonal variability influences outdoor aerosol composition (Poulain *et al.*, 2011; Talbot *et al.*, 2016) which adds further uncertainties to indoor measurements because of the influence of the phase shift of semivolatile species and the water content of hydrophilic particles (Li and Hopke, 1993; Tsai *et al.*, 2012).

Ammonium nitrate (NH_4NO_3) has received considerable attention in investigations of indoor air because of its surpringly low indoor concentrations and relative abundance in outdoor environments (Lunden *et al.*, 2003; Smolík *et al.*, 2013; Mašková *et al.*, 2015). The rate of dissociation of NH_4NO_3 is strongly correlated to temperature (Stelson and Seinfeld, 1982), interaction with physical features of the indoor environment, and sampling methods (Hering and Cass, 1999). These loss mechanisms highlight the relevance of sampling time resolution and instrument choice when sampling indoors (Zhu *et al.*, 2012; Hodas and Turpin, 2013), especially when utilising filter and impactor measurements to obtain PM_x metrics for indoor/outdoor (I/O) chemical analysis.

Here, we report on changes to aerosol particles during and after their migration from outdoor to indoor environments. When sampling from an unoccupied flat in a Central European urban background site during summer and winter, we utilised a timed switching valve to sequentially sample 10 min indoors and 10 min outdoors with an online scanning mobility particle sizer (SMPS) and an aerosol mass spectrometer (AMS). This high temporal-resolution instrumentation enabled the investigation of outdoor particles migrating indoors, which could be observed proportionally by using calculated I/O ratios. From these ratios, changes in particle size and physicochemical characteristics indoors could be identified in relation to the chemical composition outdoors, as well as physical parameters such as wind speed, temperature, and relative humidity. The online results were supported by simultaneously obtained offline BLPI measurements that provided indoor and outdoor mass size distributions and chemical analysis. We also provide detailed observations of changes in species mass in relation to sampling time resolution through comparing the 24-h BLPI measurements to the 1-min AMS results. The relevance of seasonal variability, instrument time resolution, meteorology, and air exchange rate for indoor aerosol size distribution and compositional mass is discussed.

METHODS

Measurement Site and Sampling Setup

The research was conducted from 16th August to 8th September 2014 and 5th to 24th February 2015 in an unoccupied ground floor flat located near the Institute of Chemical Process Fundamentals (ICPF; 50°7'36.47"N, 14°23'5.51"E, 277 m ASL) in Suchdol, the Czech Republic. Details of the flat location and layout are provided in Figs. SI 1(a) and 1(b), with detailed descriptions of the flat also available in previous studies by Hussein *et al.* (2006). Other studies have shown no major local emission sources close by (Ondráček *et al.*, 2011).

Suchdol is a residential area in northwestern Prague approximately 6 km north of the city centre and is recognised as an urban background site. Southerly airflows are not commonly observed at the study site; however, some recirculation of urban air and microairflow dynamics likely directs urban aerosol over the measurement site.

Within the flat, a bedroom was utilised to locate and run the online instrumentation. A 2-m inlet protruded from the bedroom into the kitchen area, 1 m away from the partitioning wall and elevated 1.5 m above the floor. The kitchen was the designated indoor sampling room for both the summer and winter phases of this study. A second 2m-long inlet sampled outdoors through a boarded-up window from the instrument room (Fig. SI 1(b)). This inlet sampled 1 m away from the building envelope and 1.5 m above the ground. A standardised sampling routine was established where indoor air was sampled for 10 min and the switching valve initiated outdoor air sampling for another 10 min. This same sampling routine was continued throughout both phases. To ensure comparability, the layout and structure of the experiment were consistent for both experiments.

Instrumentation and Data Collection

Scanning Mobility Particle Sizer

Size-resolved particle number size distribution for 14.7 to 724 nm size particles was obtained with a SMPS (model 3936, TSI, with long DMA 3081 and CPC 3775) using a 180-s up-scan, 30-s down-scan, and 90-s pause to flush the sampling train. The switching valve was timed to switch automatically between indoor and outdoor sampling every 10 min. This allowed for two full SMPS scans per sampling run. We considered only the second scan for analysis to ensure the sample represented only aerosol from its designated indoor or outdoor origin. For SMPS measurements, a particle density of 1.5 g cm^{-3} was used. The SMPS size and mass distribution data was analysed using the TSI Aerosol Instrument Manager inversion routine, applying algorithms based on the assumption that all the particles were perfect spheres.

Compact Time-of-Flight Aerosol Mass Spectrometer

The Compact Time-of-Flight Aerosol Mass Spectrometer (Aerodyne, USA) provides real-time measurements of PM_1 chemical composition and size distribution (Drewnick *et al.*, 2005). For both phases of this study, the AMS alternated between the particle time-of-flight (PToF) and mass spectra modes. Both modes applied a sampling time of 1 min over a 10-min period before switching modes. The first 2 min of each measurement mode were deleted from the dataset to avoid contamination from the previous sampling run. For the PToF mode, the aerosol beam was cut by a chopper wheel with a radial slit. Particle size information was obtained as a function of PToF in nonrefractory PM_1 (NR-PM_1). The reported mass concentrations and size distributions were then averaged. The AMS was calibrated weekly during this phase using the brute force single particle mode (Decarlo *et al.*, 2006). The collection efficiency for the AMS data was 0.7 in summer and 0.67 in winter. The results were calculated by determining the total SMPS mass and subtracting the elemental carbon mass obtained from the elemental

carbon/organic carbon (EC/OC) analysis.

Elemental Carbon/Organic Carbon

EC/OC measurements were performed using two parallel, semi-online field analysers (Sunset Laboratory Inc., USA) with $PM_{2.5}$ cyclone inlets. The instruments were equipped with a carbon parallel-plate diffusion denuder (Sunset Laboratory Inc., USA) to remove volatile organic compounds that may have caused a positive bias in the measured OC concentrations. Samples were obtained every 2 h; this included the thermal-optical analysis, which lasted for aproximately 15 min during each sample period. The analysis was performed using the shortened EUSAAR2 protocol [i.e., step (gas) temperature (°C)/duration (s)]: He 200/90, He 300/90, He 450/90, He 650/135, He-Ox. 500/60, He-Ox. 550/60, He-Ox. 700/60, and He-Ox. 850/100 (Vodička *et al.*, 2013). The collected OC was evaporated and then oxidised to CO_2 either on an MnO_2 catalyst or together with EC on the filter by oxygen in the He/Ox. phase. Analyses were then conducted using a nondispersive infrared detector. Automatic optical corrections for charring were made during each measurement and the split point between the EC and OC was detected automatically using RTCalc522 (Sunset Laboratory Inc., USA).

Berner Low Pressure Impactors

Two Berner-type low pressure impactors (BLPI, 25/0.018/2, Hauke, Austria) were run concurrently indoors and outdoors over four and five periods in the summer and winter phases of the study, respectively. The duration of all sampling periods was 24 h. The samples were captured on polycarbonate foil coated with Apiezon L vacuum grease to reduce particle bounce. Ten size fractions were separated with a flowrate of 25 L min^{-1}. The cutting sizes for samples of these impactors at each stage were quantified by Štefancová *et al.* (2011) as 0.026, 0.057, 0.1, 0.16, 0.25, 0.44, 0.87, 1.8, 3.5, and 6.7 μm.

Particle mass concentrations on impactor substrates were gravimetrically determined by pre- and postweighing the polycarbonate foils with a Sartorius M5P-000V001 electronic microbalance with a ± 1 μg sensitivity. One blank sample was collected for each 24-h sampling period, and the deviation of mass values caused by varying conditions was corrected according to the corresponding blanks. All the samples were equilibrated for a 24-h period before being weighed in a temperature- and relative humidity-controlled room. The electrostatic charges of the foils were removed using a U-shaped electrostatic neutraliser (Haug, type PRX U) and each sample was weighed three times with an accuracy of ± 2 μg. After weighing, the sampled foils were stored in a freezer at –18°C.

Ion Chromatography Analysis

Ion chromatography analysis was carried out using approximately one-third of each foil. Samples from each stage were cut and the number of aerosol spots on each cut piece was calculated. The ratio between the cut piece and total number of spots at each impactor stage was used to recalculate the results to provide an overall ion quantity for each stage. All the samples were then extracted with 7 mL of ultrapure water, sonicated for 30 min in an ultrasonic bath, and shaken for 1 h. The extracts were then analysed using a Dionex 5000 system both for cations (Na^+, NH_4^+, K^+, Ca^{2+}, and Mg^{2+}) and anions (SO_4^{2-}, NO_3^-, Cl^-) in parallel. An IonPac AS11-HC 2 × 250 mm column was applied for anions using hydroxide eluent and an IonPac CS18 2 × 250 mm was applied for cations with methane sulfonic acid solution as an eluent. Both the anion and cation setups were equipped with electrochemical suppressors. External calibration was performed using NIST traceable calibration solutions.

Meteorological Measurements

Meteorological conditions (ambient temperature, pressure, relative humidity, wind direction and velocity, and total solar radiation) were recorded by the weather station of the Czech Hydrometeorological Institute. The weather station is permanently located at the ICPF compound near the research location.

Final Data Considerations

During short periods of both summer and winter campaigns particle emissions were released from various different (mainly) indoor sources (cooking and smoking for example). The times when these controlled emission releases took place were carefully noted in a metadata file. Subsequently, all data was removed from these periods. Data was considered to be anomalous until concentrations within the room were comparable to those values before the emission source was released. No data-smoothing procedures were used during either phase of the study.

This research involves the intercomparison of different measurement results from different instruments. SMPS uses a particles mobility diameter, which, when converted to aerodynamic mobility will then cover the same range of particle sizes as the AMS. The AMS uses vacuum aerodynamic diameter to express particle size. Moreover, as shown by Figs 2, and 4 almost all our measured particles indoors and outdoors are less than 0.5 μm in diameter making particle number concentration analysis comparable between the SMPS, AMS, and EC/OC.

In regards to comparability for the different time sequencing used between the three instruments, the AMS data was integrated to match the 5 minutes scans of the SMPS whilst the Sunset 2 hour runs were held as constants over the 2-hour periods.

Air Exchange Rates during Experimentation

A controlled amount of CO_2 was emitted into the sample room and its decay curve was used as the marker for the air exchange rates (AER) in this study. Because of the location of the filter measurement instrumentation within the sample room, three such experiments were conducted.

1. Windows and doors shut, not running instrumentation in the room: 1.3 air exchanges per hour.
2. Microventilation conditions with not running instrumentation in the room: 1.9 air exchanges per hour.
3. Windows sealed and running instrumentation in the room: 1.3 air exchanges per hour.

Scenario 3 was the default set-up during both summer and winter experiments with the room remaining sealed and undisturbed except for instrument maintenance. Periods when the room was disturbed,were carefully logged and the data covering these episodes were removed.

Due to the high flowrate of the BLPI it was considered that this might have an effect on the total air exchange rate; however, this was shown not to be the case, noted by no diference in AER between scenarios 1 and 3.

During the winter campaign, the windows are unsealed for a limited time period to hasten the AER, the results of this period are described in section 3.5.

Meteorological Conditions during the Study

The mean meteorological conditions for both the winter and summer phases of the study are presented in the supplementary material (Table SI 1) with averages for the entire study.

A prolonged stable air mass was observed over Central Europe during the summer, producing only one rain event. This rain event lasted for 50 minutes and resulted in an observed change to the PNC and PSD on that day. These changes are discussed in detail in Talbot *et al.* (2016). The data collected during this rain event has been left in the dataset.

When the high pressure moved from west to east over the study period, the airflow switched from a westerly to easterly direction. This change in wind direction caused a slow increase in temperature during the final week of the study. By contrast, conditions changed more frequently in the winter, with a northerly flow at the beginning of the season changing to an easterly and then a southerly flow, and a milder westerly flow at the end of this period of research.

RESULTS AND DISCUSSION

Indoor and Outdoor Aerosol Composition Overview

Particle Size and Number Distributions

The overall particle number concentrations (PNCs) for the summer and winter phases of this studies were highly similar (Tables 1(a) and 1(b)), although subdaily seasonal differences in PNC were evident (Fig. 1). From 00:00–03:00, PNCs were found to be steadily reduced both indoors and outdoors, this is attributed mainly to decreased outdoor emissions (traffic and residential combustion). A strong morning traffic signature was evident from the increase in PNCs between 07:00–10:00. Afternoon increases in summer PNCs were attributed to new particle formation (NPF) events (Monks *et al.*, 2009; Putaud *et al.*, 2010; Zíková and Ždímal, 2013). These events did not occur daily but were represented in arithmetic mean concentrations. No NPF events were observed during the winter phase of the study. Increases in evening PNC occurred earlier in the winter than the summer because of increased input from home heating sources (Štefancová *et al.*, 2011) coupled with a lower boundary layer height and possible temperature inversions. Conversely, the corresponding later increase during summer was a product of a higher boundary layer which increased mixing, as well as a possible reformation of particle nitrate through lowering temperatures (Kubelová *et al.*, 2015). Notably, total I/O concentrations diverged after 16:00 during the winter (Fig. 1). We attribute this to an increased ultrafine mode resulting from home heating combustion. The ultrafine fraction has been found to penetrate with comparatively lower effectiveness because of diffusive processes on building surfaces (Nazaroff, 2004).

Average particle size distributions during summer revealed

Table 1(a). Results from the summer phase of this study, including the mean, maximum, and standard deviation (σ).

Instrument	Species	Summer Outdoors			Summer Indoors		
		Mean	Max	σ	Mean	Max	σ
(EC-OC)	EC (μg m^{-3})	0.95	2.5	0.4	0.8	5.2	0.4
AMS	Org (μg m^{-3})	3.6	15.3	1.5	2.7	7.9	1.3
AMS	SO_4^{2-} μg m^{-3})	2.1	5	1.1	1.7	4.4	0.9
AMS	NH_4^+ (μg m^{-3})	0.5	1.1	0.2	0.3	0.6	0.1
AMS	NO_3^- (μg m^{-3})	0.9	2.8	0.5	0.5	2	0.5
SMPS	Total number (pp cm^{-3})	5.5×10^3	2.8×10^4	3.1×10^3	3.1×10^3	1.1×10^4	1.4×10^3
SMPS	Total mass (μg m^{-3})	6.4	15.9	2.9	3.7	9.7	1.2
AMS	Total mass (μg m^{-3})	7.1			5.2		

Table 1(b). Results from the winter phase of this study, including the mean, maximum, and standard deviation (σ).

Instrument	Species	Winter Outdoors			Winter Indoors		
		Mean	Max	σ	Mean	Max	σ
(EC-OC)	EC (μg m^{-3})	1.4	6	0.9	1.3	4.7	0.8
AMS	Org (μg m^{-3})	8.2	42.8	6.6	4.4	18.5	3.4
AMS	SO_4^{2-} (μg m^{-3})	4	14.1	2.9	2	12.3	1.6
AMS	NH_4^+ (μg m^{-3})	3.2	10.5	2.2	0.9	4.5	0.7
AMS	NO_3^- (μg m^{-3})	7.2	29.6	6	1.4	8.2	1.2
SMPS	Total number (pp cm^{-3})	5.4×10^3	2.9×10^4	3.1×10^3	3.0×10^3	1.8×10^4	1.9×10^3
SMPS	Total mass (μg m^{-3})	15.7	52.6	8.8	8.1	24.6	5.2
AMS	Total mass (μg m^{-3})	22.6					

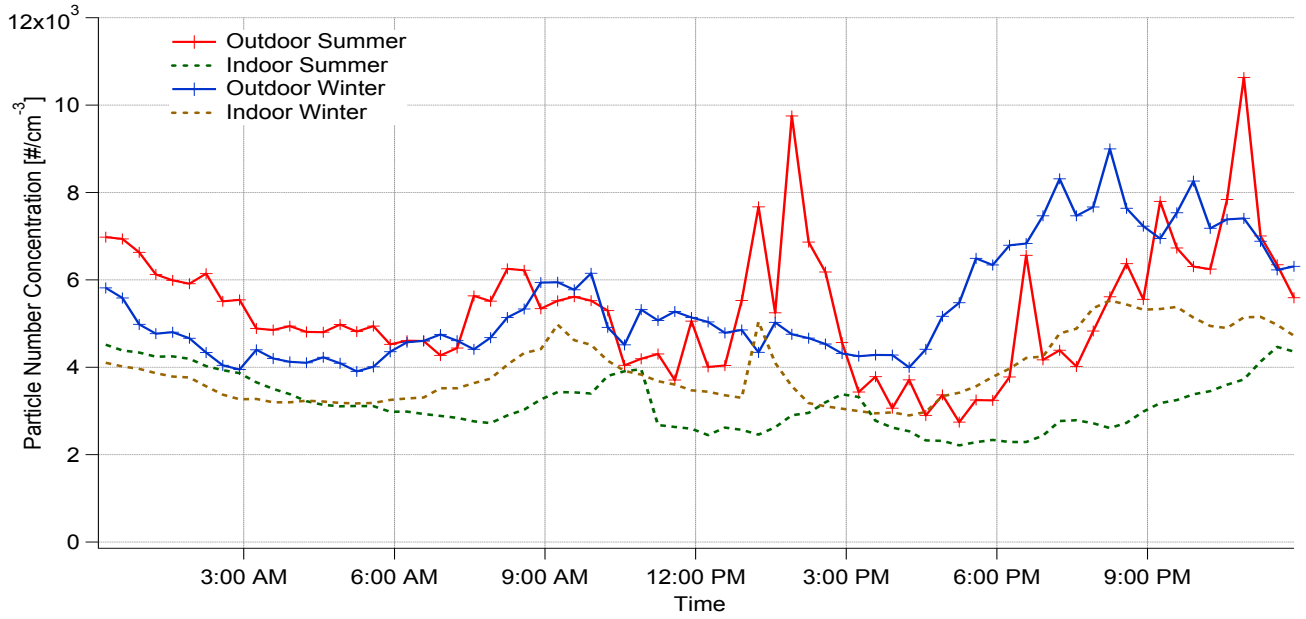

Fig. 1. Arithmetic mean PNC measured by the SMPS, relative to the time of day and season.

a prominent outdoor mode between 20–30 nm (Fig. 2). This mode has been described in previous research as an indicator of fresh exhaust emissions (Ristovski *et al.*, 1998) and secondary aerosol resulting from (NPF) events.

A second mode between 50–60 nm during the summer and 50–80 nm during the winter was observed. These ranges are typical of aged coagulated combustion emissions; larger sizes are attributed to diesel emissions, which have been shown to produce particulates between 50–120 nm (Ondráček *et al.*, 2011). Accumulation mode peaks were evident for both summer and winter; these were most likely the product of secondary inorganics and other regional transported aerosol sources (Lehmann *et al.*, 2005). Indoor modes were less pronounced than those outdoors, which was further evidence of the poor penetration of the ultrafine modes compared to accumulation modes caused by diffusion processes on building surfaces (Zhu *et al.*, 2005).

Chemical Analysis from AMS Measurements

Indoor and outdoor chemical composition masses separated to represent summer and winter are shown in Tables 1(a) and 1(b). The proportional chemical compositions are presented in Fig. 3. During winter, proportionally lower percentages of NR-organics were observed outdoors (winter: 36%; summer: 51%); this can be attributed to the increases in concentrations of other inorganic species such as NO_3^- and NH_4^+ during this period. The outdoor share of NO_3^- significantly decreased from winter to summer (winter: 32%; summer: 13%); this can be explained by the lower temperatures in winter supporting the aerosol phase of NH_4NO_3 over the gaseous phase (Stelson and Seinfeld, 1982; Huang *et al.*, 2004; Poulain *et al.*, 2011). In addition, this phase transformation was responsible for the low concentrations of NO_3^- observed indoors during both seasons, with higher constant average temperatures indoors, lower relative humidity, and HNO_3 acid–surface reactions all acting to increase dissociation rates (Hering and Cass, 1999; Smolík *et al.*, 2008).

NH_4^+ (winter: 14%; summer: 7%), is the principal base in the atmosphere and acts primarily to neutralise SO_4^{2-} and, to a lesser extent, NO_3^-. Hence, assuming that NH_4^+ concentrations would be closely correlated to the concentrations of those species was reasonable; however, this was not observed in our results, which showed NH_4^+ mass concentrations lower than both NO_3^- and SO_4^{2-}. The reduction in the proportional share of SO_4^{2-} outdoors during winter (winter: 18%; summer: 29%) was most likely a result of a decrease in daily mixing height during the cool winter months, with lower mixing height restricting the input of SO_4^{2-} from the boundary layer reservoir (Kvietkus *et al.*, 2011) and reducing regional SO_4^{2-} contributions. Similarly, lower light intensity during the winter reduced the photo-oxidation of SO_2 (Querol *et al.*, 1998).

Outdoor chemical mass concentrations from the summer and winter phases of the study were within the standard deviation of results described by Kubelová *et al.* (2015), where NR-PM_1 levels were measured during summer 2012 and winter 2013 in the Czech Republic. In that study, NR-organics dominated during both winter and summer, with NO_3^- being the second most abundant aerosol outdoors during winter and SO_4^{2-} the second most abundant during summer. We observed a higher concentration of NR-organics and SO_4^{2-} in both seasons; however, this difference was within the range set by the standard deviation. The same observation applies to the measured concentrations of NO_3^- and NH_4^+ in summer; whereas in winter our measured concentrations of NO_3^- and NH_4^+ were lower than those described in Kubelova *et al.* (2015). However, they were also within the range set by the standard deviation.

I/O BLPI Measurements

Two BLPIs provided the concurrent indoor and outdoor mass size distributions of the major ions (SO_4^{2-}, NH_4^+, and

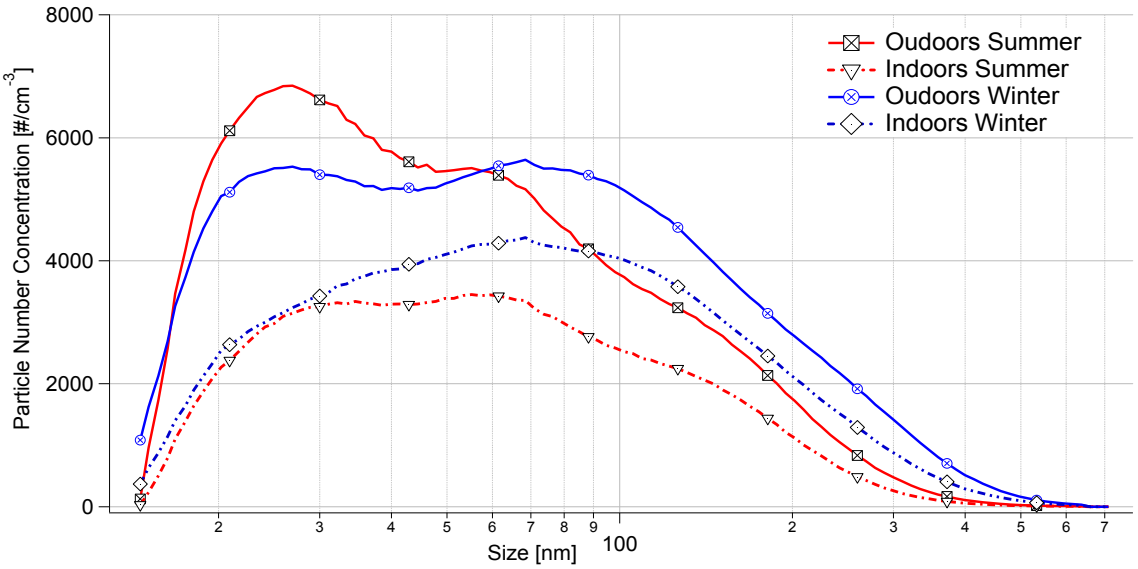

Fig. 2. Average indoor and outdoor particle number concentrations and size modes from the summer and winter phases of this study.

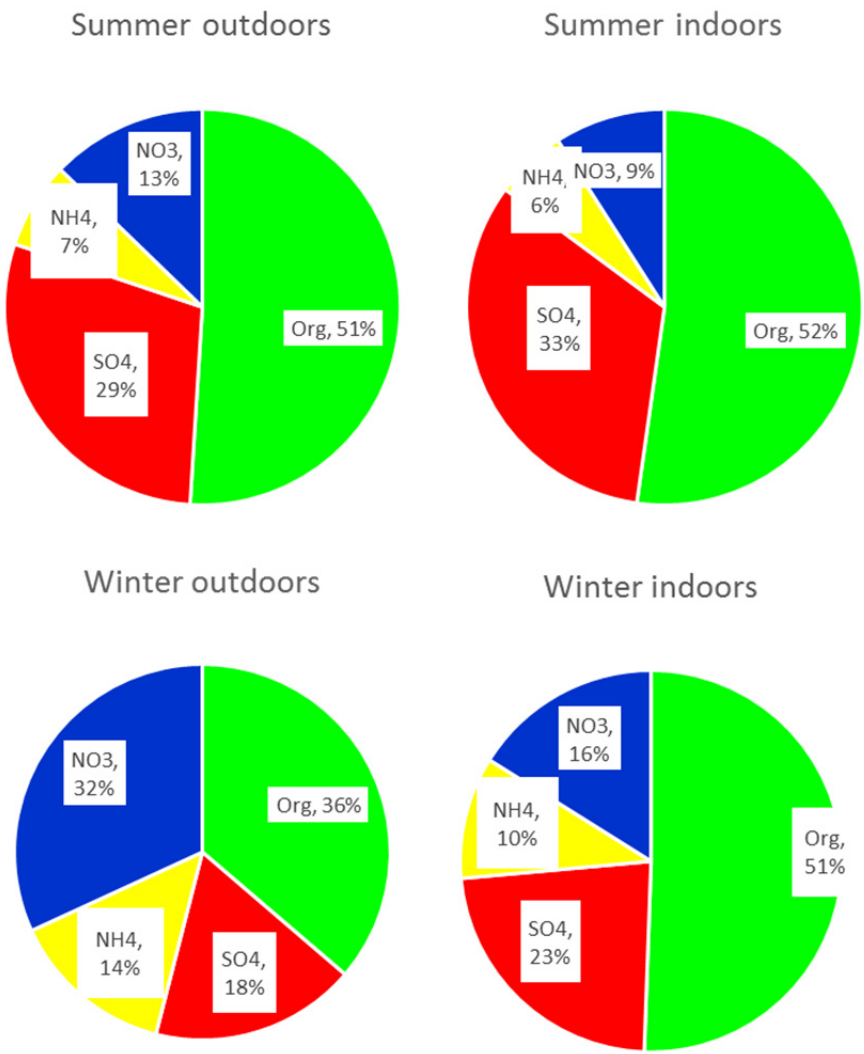

Fig. 3. Averaged indoor and outdoor proportional chemical composition in winter (below) and summer (above) measured using the AMS.

NO_3^-) for 25-nm to 10-µm particle sizes. The overall mean mass concentrations for SO_4^{2-}, NH_4^+, and NO_3^- are presented in Figs. 4(A), 4(B), and 4(C), respectively. The mean particle size distribution was smaller in summer (340-nm median stage size) than in winter (650-nm median stage size). We ascribe this change to seasonal differerences (longer daylight hours and warmer temperatures during summer) in aerosol composition as well as changes in the water content of the hydrophilic particles (Table SI 1). This result supports the findings of Schwarz *et al.* (2012), who described seasonal and airmass effects in detail.

A larger concentration of < 200 nm mass particles was recorded on the indoor BLPI for both SO_4^{2-} and NH_4^+. This anomaly was more pronounced during the winter phase of the study, in which particle mass concentrations indoors were nearly double those outdoors on the last 4 BLPI stages, which accounted for the < 200 nm particle mass. No known indoor sources that could have generated the extra mass were present, and particle bounce-off from the higher stages can be ignored because of the greasing of our polycarbonate foils. Hence, the higher indoor mass of these smallest stage particles can be explained by water soluble outdoor aerosol particles drying and shrinking as they entered the warmer and drier indoor environment. This process is produced by water molecules rapidly evaporating from the surface or core of a particle when the particle enters the indoor environment, thereby equilibrating the vapour pressure of the water on the particle to that of the atmospheric conditions

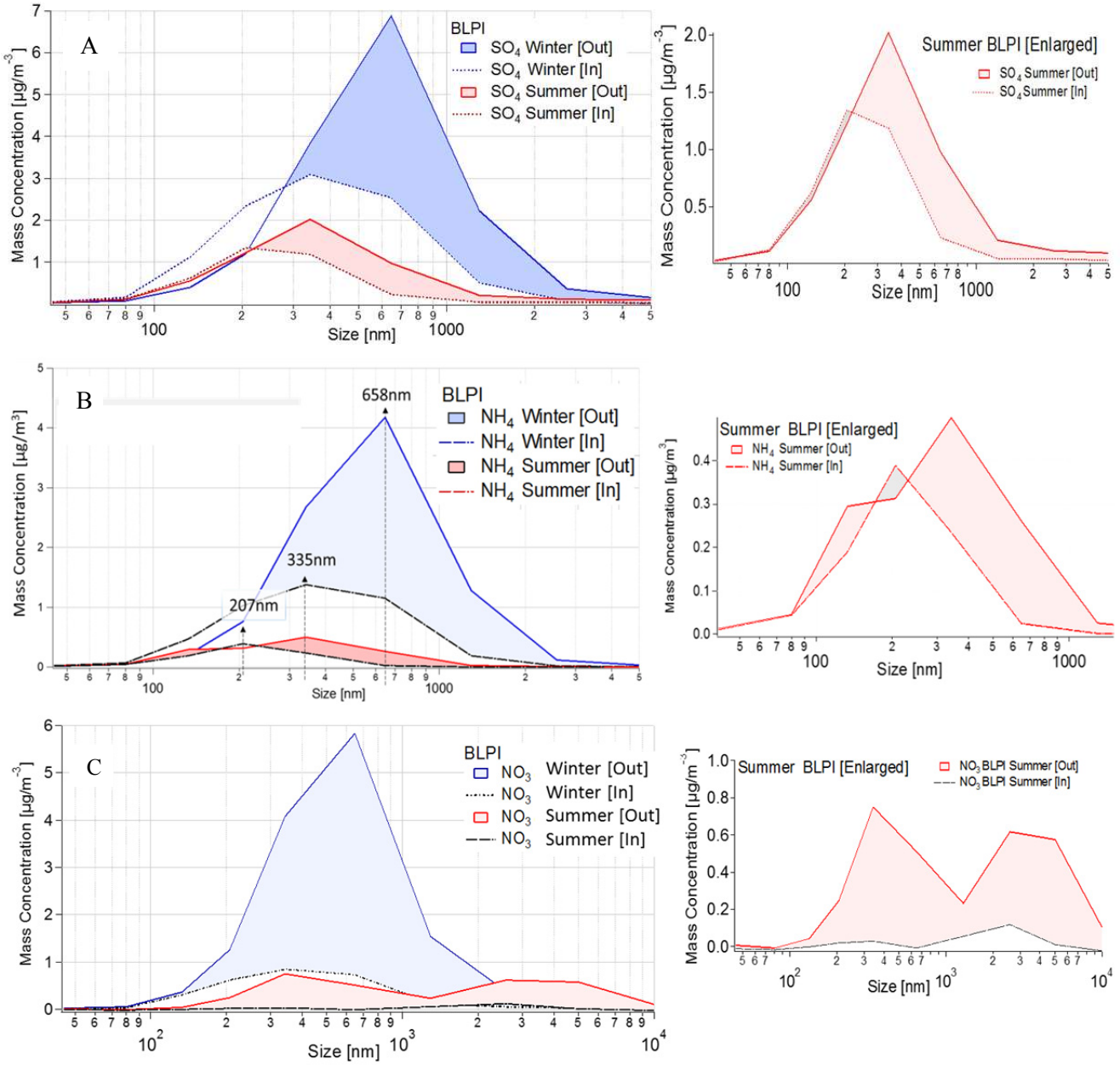

Fig. 4. Graphical representation of the winter and summer BLPI particle mass size distributions for (A) SO_4, (B) NH_4, and (C) NO_3. The summer data for all results are shown in proportional scale and also enlarged as a subplot.

indoors (Lunden *et al.*, 2003; Seinfeld and Pandis, 2012). The mean temperature gradient from outdoors to indoors during winter was 21.2°C (calculated by dividing the average temperatures indoors and outdoors) compared to 1.7°C during the summer. These averages neglected the diurnal variation in temperatures that occurs outdoors during both seasons, but nevertheless highlighted the relevance of the temperature difference between indoor and outdoor environments when comparing I/O particle size distributions.

During winter, NO_3^- (Fig. 4(C)) largely mirrored the mass size distribution results of the SO_4^{2-} and NH_4^+ outdoors. However, NO_3^- lost considerably more mass indoors than any other measured chemical species. This increased loss can be attributed to an increase in the rate of the dissociation of NH_4NO_3 (probably the most prevalent chemical form for NO_3^-) indoors because of higher temperatures, lower relative humidity, and greater surface reactions. Moreover, the loss was exaggerated by the higher concentrations of NH_4NO_3 outdoors during the winter study because of the predominantly cool, damp conditions. Notably, during the summer study the BLPI recorded negligible NO_3^- mass indoors, in contrast to the proportional observation of 9% NO_3^- produced by the AMS measurements. This can be explained with near certainty by the difference in the sampling time, namely a 1-min time resolution for the AMS measurements and a 24-h sampling period for the BLPI.

Finally, NO_3^- was found to have a distinct coarse mode. This is the likely product of NaCl originating from maritime sources, which becomes enriched with NO_3^- as the air mass passes over the European continental landmass, the end chemical product being $NaNO_3$. These results also support those described by Schwarz *et al.* (2012).

I/O Ratios

In the absence of indoor aerosol sources, indoor concentrations are known to be correlated to the concentrations outdoors through the migration of outdoor aerosol indoors (Hussein *et al.*, 2006). Aerosol particles can penetrate through windows, structures, building envelopes, and ventilation mechanisms. Following Chen and Zhao (2011) this process can be characterised by an Indoor/Outdoor (I/O) ratio, expressed as

$$\text{I/O Ratio} = \frac{C\_in}{C\_\text{out}} \quad (1)$$

I/O Ratios and Particle Number Concentration

The median I/O ratios based on PNC are shown in Fig. 5 (boxplots 1–3 on the left) and have been subdivided into nucleation, Aitken, and accumulation modes. The nucleation and Aitken modes were similar for both seasons; but the accumulation modes behaved differently between summer and winter, supporting the findings from the BLPI mass size distribution data discussed in section 3.2. The shrinkage of the accumulation mode particles may increase the membership, and therefore the ratio, of the Aitken and nucleation modes; however, this process is not apparent in the boxplots.

To further explore these results, linear regression models were created using the same 3-size modes, placing indoor data on the Y-axis and outdoor data on the X-axis. The results are graphed in Fig. 6, together with the calculated correlation R^2 and slope values, which are representative of the I/O ratios. For summer, the nucleation mode (< 40 nm) exhibited a highly scattered and disordered relationship, whereas the

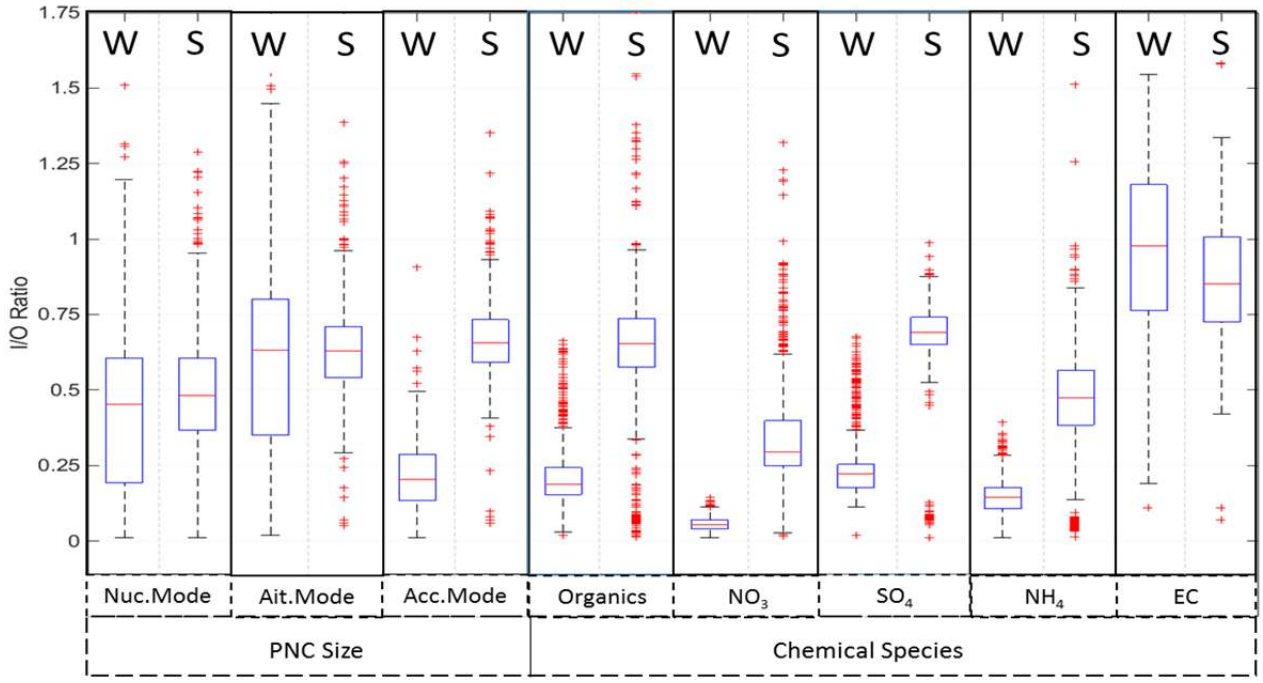

Fig. 5. Boxplots showing the averaged I/O ratio for PNC using SMPS and chemical PM_1 data from AMS and EC/OC measurements separated into winter (W) and summer (S) segments. The red line is the median value and the edge of the box represents the 25th and 75th percentiles. The whiskers show the 5th and 95th percentiles and the crosses denote outliers.

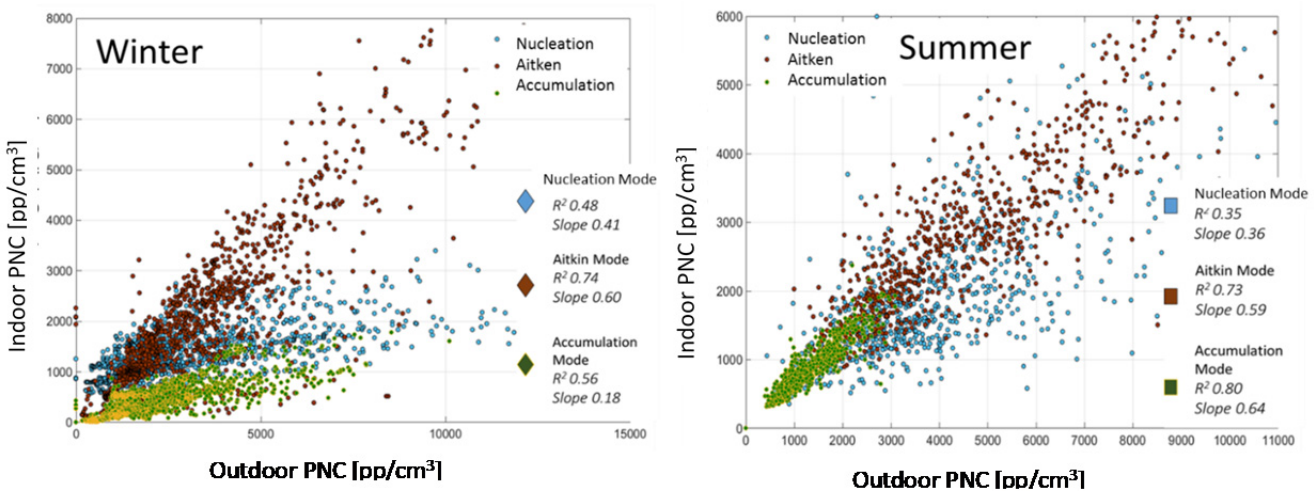

Fig. 6. Linear regression models for PNC split into three size modes and separated into summer and winter. Data measured using the SMPS.

Aitken and accumulation modes showed a high correlation between indoors and outdoors. The accumulation modes were strongly correlated and produced a slope of 0.64, which is in close agreement with Fig. 5. For winter, the nucleation mode slope was higher than that for summer; this can be attributed to the shrinkage of larger particles. However, Aitken mode fractions for the two seasons were highly similar, albeit with more scatter for summer than winter. By contrast, wintertime I/O accumulation modes were weakly correlated and a corresponding slope of 0.18 revealed an extremely low I/O ratio. These results provide further evidence of the shrinking process of indoor aerosol particles.

I/O Ratios and Chemical Composition

The I/O ratios were calculated by comparing the chemical mass composition results with the indoor and outdoor AMS measurements. These reveal a decrease in the I/O ratios for all measured chemical species (Fig. 5). The mean I/O ratios (winter/summer) for each species were NR-organics (.47/.72), NO_3^- (.20/.32), SO_4^{2-} (.49/.76), and NH_4^+ (.31/.48). Based on these results, the seasonal decrease in the I/O ratio was NR-organic (34.7%), NO_3^- (37.5%), SO_4^{2-} (35.5%), and NH_4^+ (35.4%). The similar seasonal I/O ratio change exhibited by all species implies that physical factors, not physicochemical processes, were primarily responsible for these differences.

The EC results revealed only a small difference in the I/O ratio between the seasons. However, the I/O values for the summer were lower, in direct contrast to the the ion species results. This was most likely because of the nonsoluble composition and low volatility of EC, which reduces the influence of physical factors such as temperature and relative humidity. However, the outdoor sampling EC/OC instrument was not kept in the main research building (Fig. SI 1). Hence, the outdoor sampling EC/OC instrument may have received different concentrations than the indoor sampling EC/OC instrument during certain periods of the study.

I/O Ratios and Wind Speed and Direction

A Spearman rank correlation statistical analysis of the winter results was performed to identify the physical factors affecting I/O ratios. The main outcome was the negative correlation between the wind speed and concentrations of all the chemical species, both indoors and outdoors. However, we have not observed any correlation between the wind speed and the I/O ratio itself. For this analysis, we only considered the winter phase of the study because of a low number of summer datapoints and the low variability in wind speed and direction during summer; however, the results should be applicable for all seasons. Notably, the presence of buildings in the vicinity is likely to have caused some microcirculation of the airflow around the sample area; all of the discussed wind speeds and directions are averaged over 1-h periods.

The influence of wind direction and wind speed on the I/O ratio is shown in Fig. 7. Higher I/O ratios were observed mainly in connection with the northeast and southwest wind directions, which were also connected with relatively higher wind speeds, i.e., over 3 m s^{-1}. However, in the case of the south east wind direction, the high I/O ratio might be caused partially by the relatively low values of both outdoor and indoor concentrations. In that case, a relatively small decrease of outdoor concentration, together with a time lag between changes in the outdoor and indoor concentration might lead to a relatively high increase in the ratio. The time lag might also explain the variability between the I/O ratio of a particular species and partially the high I/O ratio connected with the north east direction (Fig. 7). Furthermore, the relatively small concentrations outdoors and indoors connected with the south west wind direction (in which case wind speeds reached up to over 4 m s^{-1}) are in compliance with the negative correlation between wind speed and pollutant concentration mentioned above. Moreover, higher wind speed might also increase the ventilation rate leading to higher I/O ratios.

The I/O ratios are likely to have been influenced by changes in aerosol particle concentrations and composition outdoors caused by wind speed and wind direction variability.

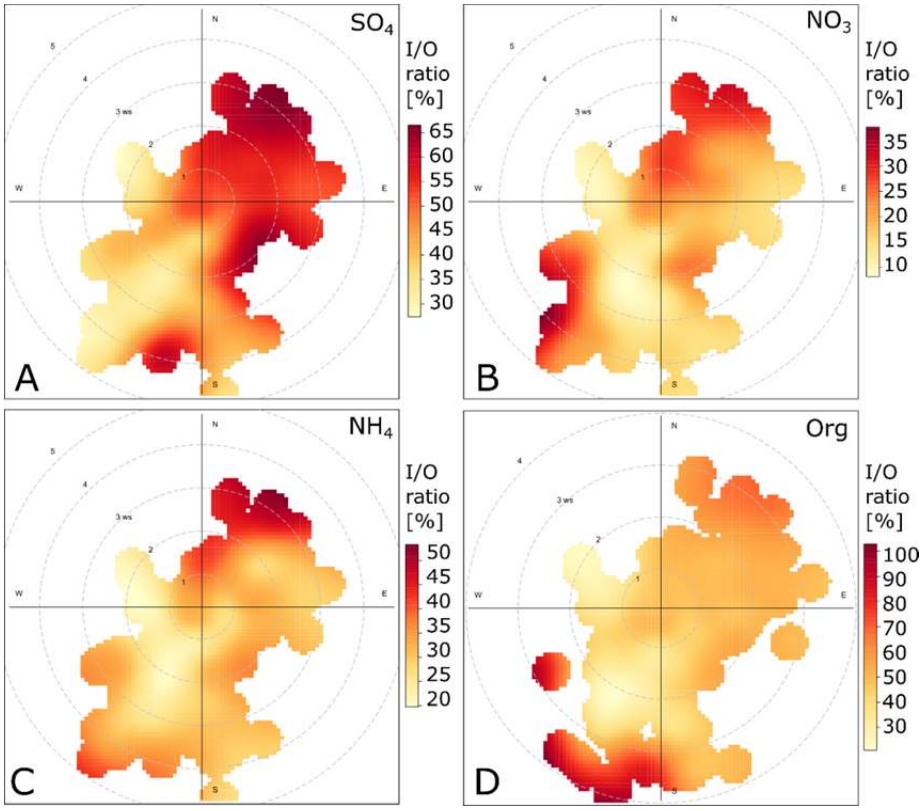

Fig. 7. Polar plots of I/O ratio (as a percentage) per species : A) SO_4, B) NO_3, C) NH_4, and D) NR-Org measured using the AMS.

Higher wind speeds decreased aerosol concentrations, and higher variability in wind speeds during winter resulted in greater fluctuation in the I/O ratios because of a time lag effect on the indoor concentrations.

Microventilation, I/O Ratios, and Chemical Compositional Changes

For a 2-day period of the winter phase of the study, the window of our sample room was unsealed. This was achieved by moving the handle of the window into an upright position from a right-angle sealed position. The result of this action was a 63% increase in the air exchange rate when compared to the sealed position (from 1.3 to 1.9 exchanges per hour) allowing for a "fresher" indoor sample with less residence time indoors and providing a useful transition point between the outdoor and indoor compositions. During the microventilation period, the average temperature in the indoor sample room dropped from 20°C to 17.2°C.

The I/O ratio for NO_3^- increased substantially during the microventilation period, with the largest increase recorded for the < 200 nm (median) stages (Fig. 8). For each of these four lowest stage sizes, the indoor mass concentrations exceeded those outdoors, causing the I/O ratio to exceed 1. SO_4^{2-} and NH_4^+ also increased their I/O ratios; notably, increases were recorded for coarse mode particles, which was indicative of the faster air exchange, allowing for these larger particles to be sampled before gravitational settling could occur.

The results from the BLPI were compared with the I/O ratios derived from the NR-PM_1 AMS measurements for the same time period (Fig. 8(B)). These show a doubling of the NO_3^- I/O ratio during microventilation; a similar increase was found for NH_4^+, indicating an increased presence of NH_4NO_3. Although the microventilation experiment was only carried out for a 2-day period, the acceleration in air exchange appears to have caused a large increase in semivolatile NH_4NO_3. However, we cannot discern whether the reduction of temperature or the increase in the ventilation rate had the greater effect on concentration. Additional experiments on adjusting temperature and air exchange rates are desirable to resolve this uncertainty. According to our observations, the increase in air exchange rate probably enabled more NH_4NO_3 to enter the room and the reduced temperature indoors allowed for the preservation of a more substantial concentration of NH_4NO_3 on the BLPI foils.

CONCLUSIONS

The overall PNCs for summer and winter were similar despite seasonal differences in sources and sinks acting to increase and reduce PNC during specific periods of the day. Size-resolved PNC exemplified these differences, exhibiting afternoon increases during summer (secondary organic aerosol and NPF) and early evening increases (home heating and low mixing layers) during winter. The observed averaged daily outdoor modes displayed a trimodal structure typical of an urban background site. Indoors, a dominant broad mode between 70 and 100 nm was found. Smaller modes

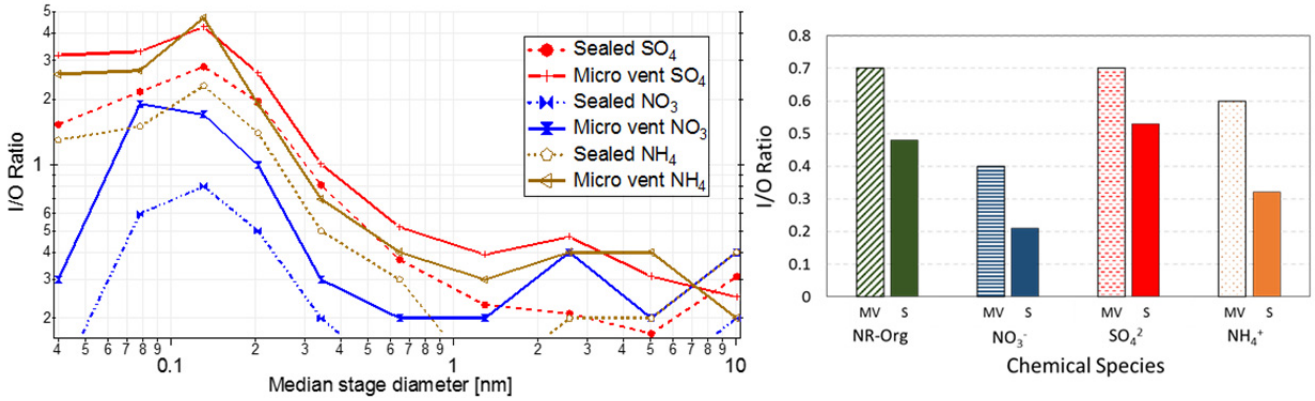

Fig. 8. Changes in I/O ratio during microventilation (MV) and sealed (S) periods from: (left) the BLPI data and (right) the AMS data.

were considerably less defined indoors than outdoors, which was attributed to the ultrafine particles diffusing onto building surfaces.

The BLPI mass size distribution results showed larger mass concentrations indoors than outdoors for < 200 nm particles, with this finding most prominent for SO_4^{2-} concentrations during the winter phase of the study. Because indoor sources and particle bounce could be discounted, this result was explained by indoor aerosol particles shrinking to smaller sizes. We attribute this wintertime shrinkage to the process of aqueous or semi-aqueous particles dehydrating as they traveled from a cool and humid environment outdoors to a warmer and drier environment indoors. The temperature and relative humidity gradients from outdoors to indoors were greater in the winter than in the summer, and the steepness of this gradient likely drove the shrinking process. Particle shrinkage was also observed in the SMPS measurements, which revealed a significant decrease in the winter I/O ratio for 100- to 700-nm mobility diameter accumulation mode particles when compared to the summer results.

A substantial reduction in indoor mass concentration was observed for all aerosol chemical species during the winter phase of the study, which could not be fully accounted for by particle drying. A decrease in I/O ratios of between 34–38% for all of the species during the winter was attributed to physical factors affecting all species rather than chemical processes acting upon each chemical species individually. This result was surprising considering the observed loss of NO_3^- indoors through dissociation caused by the temperature and relative humidity changes. Despite NO_3^- being much more prevalent outdoors during winter, the relative loss of mass, implied by I/O ratio changes, apparently did not change substantially according to the season.

A nonparametric statistical test was used to assess the significance of numerous nonchemical factors influencing the outdoor and indoor chemical composition. These tests identified wind speed to be negatively correlated with outdoor and indoor concentrations, with polar plots revealing certain dependence of the indoor and outdoor concentrations on the wind speed and direction. We do not believe that wind speed and wind direction are the primary loss mechanism for indoor mass, but rather only a factor that combines with the I/O temperature gradients, relative composition of outdoor aerosol, and air exchange rate from the indoor sample location.

ACKNOWLEDGEMENTS

The authors acknowledge support provided for this research by the European Union Seventh Framework Programme (FP7/2007–2013) under grant agreement no. 315760 HEXACOMM.

SUPPLEMENTARY MATERIAL

Supplementary data associated with this article can be found in the online version at http://www.aaqr.org.

REFERENCES

Andelova, L., Smolik, J., Ondrackova, L., Ondracek, J., Lopez-Aparicio, S., Grontoft, T. and Stankiewicz, J. (2010). Characterization of airborne particles in the Baroque hall of the National Library in Prague. *e-Preservation Sci.* 7: 141–146.

Brauer, M., Koutrakis, P., Keeler, G. and Spengler, J. (1991). Indoor and outdoor concentrations of inorganic acidic aerosols and gases. *J. Air Waste Manage. Assoc.* 41: 171–81.

Buzea, C., Pacheco, I. and Robbie, K. (2007). Nanomaterials and nanoparticles: Sources and toxicity. *Biointerphases* 2: MR17–MR71.

Chen, C. and Zhao, B. (2011). Review of relationship between indoor and outdoor particles: I/O ratio, infiltration factor and penetration factor. *Atmos. Environ.* 45: 275–288.

Colbeck, I., Nasir, Z.A. and Ali, Z. (2010). The state of indoor air quality in pakistan--A review. *Environ. Sci. Pollut. Res.* 17: 1187–1196.

Dawson, M.L., Varner, M.E., Perraud, V., Ezell, M.J., Gerber, R.B. and Finlayson-Pitts, B.J. (2012). Simplified mechanism for new particle formation from methanesulfonic acid, amines, and water via experiments

and ab initio calculations. *Proc. Natl. Acad. Sci. U.S.A.* 109: 18719–18724.

Decarlo, P., Kimmel, J., Trimborn, A., Northway, M.J., Jayne, J.T., Aiken, A.C. and Gonin, M. (2006). Aerosol mass spectrometer. *Anal. Chem.* 78: 8281–8289.

Diapouli, E., Eleftheriadis, K., Karanasiou, A., Vratolis, S., Hermansen, O., Colbeck, I and Lazaridis, M. (2011). Indoor and outdoor particle number and mass concentrations in Athens. Sources, sinks and variability of aerosol parameters. *Aerosol Air Qual. Res.* 11: 632–642.

Drewnick, F., Hings, S.S., DeCarlo, P., Jayne, J., Gonin, M., Fuhrer, K. and Weimer, S. (2005). A new time-of-flight aerosol mass spectrometer (TOF-AMS)—Instrument description and first field deployment. *Aerosol Sci. Technol.* 39: 637–658.

Guo, H., Morawska, L., He, C. and Gilbert, D. (2008). Impact of ventilation scenario on air exchange rates and on indoor particle number concentrations in an air-conditioned classroom. *Atmos. Environ.* 42: 757–768.

Guo, H., Morawska, L., He, C., Zhang, Y,. Ayoko, G. and Cao, M. (2010). Characterization of particle number concentrations and $PM_{2.5}$ in a school: Influence of outdoor air pollution on indoor air. *Environ. Sci. Pollut. Res. Int.* 17: 1268–1278.

Hämeri, K., Hussein, T., Kulmala, M. and Aalto, P. (2004). Measurements of fine and ultrafine particles in Helsinki: Connection between outdoor and indoor air quality. *Boreal Environ. Res.* 9: 459–467.

Han, Y., Li, X., Zhu, T., Lv, D., Chen, Y., Hou, L., Zhang, Y. and Ren, M. (2016). Characteristics and relationships between indoor and outdoor $PM_{2.5}$ in Beijing: A residential apartment case study. *Aerosol Air Qual. Res.* 16: 2386–2395.

Hering, S. and Cass, G. (1999). Magnitude of bias in the measurement of $PM_{2.5}$ arising from volatilization of particulate nitrate from Teflon filters. *J. Air Waste Manage. Assoc.* 49: 725–733.

Hering, S.V., Lunden, M.M., Thatcher, T., Kirchstetter, T.W. and Brown, N.J. (2007). Using regional data and building leakage to assess indoor concentrations of particles of outdoor origin. *Aerosol Sci. Technol.* 41: 639–654.

Hodas, N. and Turpin, B.J. (2013). Shifts in the gas-particle partitioning of ambient organics with transport into the indoor environment. *Aerosol Sci. Technol.* 48: 271–281.

Hsu, Y.C., Kung, P.Y., Wu, T.N. and Shen, Y.H. (2012). Characterization of indoor-air bioaerosols in Southern Taiwan. *Aerosol Air Qual. Res.* 12: 651–661.

Huang, H., Lee, S.C., Cao, J.J., Zou, C.W., Chen, X.G. and Fan. S.J. (2007). Characteristics of indoor/outdoor $PM_{2.5}$ and elemental components in generic urban, roadside and industrial plant areas of Guangzhou City, China. *J. Environ. Sci.* 19: 35–43.

Huang, Z., Harrison, R.M., Allen, A.G., James, J.D., Tilling, R.M. and Yin, J. (2004). Field intercomparison of filter pack and impactor sampling for aerosol nitrate, ammonium, and sulphate at coastal and inland sites. *Atmos. Res.* 71: 215–232.

Hussein, T., Hameri, K., Aalto, P., Asmi, A., Kakko, L. and Kulmala, M. (2004). Particle size characterization and the indoor-to-outdoor relationship of atmospheric aerosols in Helsinki. *Scand. J. Work Environ. Health* 30: 54–62.

Hussein, T., Glytsos, T., Ondráček, J., Dohányosová, P., Ždímal, V., Hämeri, K., Lazaridis, M., Smolík, J. and Kulmala, M. (2006). Particle size characterization and emission rates during indoor activities in a house. *Atmos. Environ.* 40: 4285–4307.

Kubelová, L., Vodička, P., Schwarz, J., Cusack, M., Makeš, O., Ondráček, J. and Ždímal, V. (2015). A study of summer and winter highly time-resolved submicron aerosol composition measured at a suburban site in Prague. *Atmos. Environ.* 118: 45–57.

Kvietkus, K., Šakalys, J., Rimselyte, I., Ovadnevaite, J., Remeikes, V. and Špakauska, V. (2011). Characterization of aerosol sources at urban and background sites in Lithuania. *Lith. J. Phys.* 51: 65–74.

Lazaridis, M., Aleksandropoulou, V., Smolík, J., Hansen, J.E., Glytsos, T., Kalogerakis, N. and Dahlin, E. (2006). Physico-chemical characterization of indoor/outdoor particulate matter in two residential houses in Oslo, Norway: Measurements overview and physical properties – URBAN-AEROSOL Project. *Indoor Air* 16: 282–295.

Lazaridis, M. and Aleksandropoulou, V. (2008). Sources and variability of indoor and outdoor gaseous aerosol precursors (O_3, NO_x and VOCs). *Water Air Soil Pollut. Focus* 9: 3–13.

Lehmann, K., Massling, A., Tilgner, A., Mertes, S., Galgon, D. and Wiedensohler, A. (2005). Size-resolved soluble volume fractions of submicrometer particles in air masses of different character. *Atmos. Environ.* 39: 4257–4266.

Leung, D.Y.C. and Drakaki, E. (2015). Outdoor-indoor air pollution in urban environment: Challenges and opportunity. *Front. Environ. Sci.* 2: 1–7.

Levy, J., Jane, I., Clougherty, E., Baxter, L.K., Houseman, A.E. and Paciorek, C.J. (2010). Evaluating heterogeneity in indoor and outdoor air pollution using land-use regression and constrained factor analysis. *Res. Rep. Health Eff. Inst.* 152: 5–80.

Li, W. and Hopke, P.K. (1993). Initial size distributions and hygroscopicity of indoor combustion aerosol particles. *Aerosol Sci. Technol.* 19: 305–316.

Long, C.M., Suh, H.H., Catalano, P.J. and Koutrakis, P. (2001). Using time- and size-resolved particulate data to quantify indoor penetration and deposition behavior. [erratum Appears in Environ Sci Technol 2001 Nov 15;35(22):4584]. *Environ. Sci. Technol.* 35: 2089–2099.

Lunden, M M., Kenneth L., Revzan, M.L., Fischer, T.L., Thatcher, D.L., Hering, S. and Brown, N.J. (2003). The transformation of outdoor ammonium nitrate aerosols in the indoor environment. *Atmos. Environ.* 37: 5633–5644.

Lunden, M.M., Kirchstetter, T.W., Thatcher, T.L., Hering, S.V. and Brown, N.J. (2008). Factors affecting the indoor concentrations of carbonaceous aerosols of outdoor origin. *Atmos. Environ.* 42: 5660–5671.

Mašková, L., Smolík, J. and Vodička, P. (2015).

Characterisation of particulate matter in different types of archives. *Atmos. Environ.* 107: 217–224.

Monks, P.S., Granier, C., Fuzzi, S., Stohl, A., Williams, M.L., Akimoto, H. and Amann, M. (2009). Atmospheric composition change – Global and regional air quality. *Atmos. Environ.* 43: 5268–5350.

Morawska, L., He, C., Hitchins, J., Gilbert, D. and Parappukkaran, S. (2001). The relationship between indoor and outdoor airborne particles in the residential environment. *Atmos. Environ.* 35: 3463–3473.

Morawska, L., He, C. and Hitchins, J. (2003). Characteristics of particle number and mass concentrations in residential houses in Brisbane, Australia. *Atmos. Environ.* 37: 4195–4203.

Nazaroff, W.W. (2004). Indoor particle dynamics. *Indoor Air* 14: 175–183.

Ondráček, J., Schwarz, J., Ždímal, V., Andělová, L., Vodička, P., Bízek, V., Tsai, C.J, Chen, S.C. and Smolík, J. (2011). Contribution of the road traffic to air pollution in the Prague city (busy speedway and suburban crossroads). *Atmos. Environ.* 45: 5090–5100.

Perez-Padilla, R., Schilmann, A. and Riojas-Rodriguez, H. (2010). Respiratory health effects of indoor air pollution. *Int. J. Tuberc. Lung Dis.* 14: 1079–1086.

Pope, C.A. and Dockery, D.W. (2006). Health effects of fine particulate air pollution: Lines that connect. *J. Air Waste Manage. Assoc.* 56: 709–742.

Poulain, L., Spindler, G., Birmili, W., Plass-Dülmer, C., Wiedensohler, A. and Herrmann, H. (2011). Seasonal and diurnal variations of particulate nitrate and organic matter at the IfT research station Melpitz. *Atmos. Chem. Phys.* 11: 12579–12599.

Pramod K., Baron, P. and Willeke, K. (2011). *Aerosol Measurement: Principles, Techniques, and Applications*. John Wiley & Sons.

Putaud, J.P., Van Dingenen, R., Alastuey, A., Bauer, H., Birmili, W., Cyrys, J. and Flentje, H. (2010). A European aerosol phenomenology – 3: Physical and chemical characteristics of particulate matter from 60 rural, urban, and kerbside sites across Europe. *Atmos. Environ.* 44: 1308–1320.

Querol, X., Alastuey, A., Puicercus, J.A., Mantilla, E., Miro, J.V., Lopez-Soler, A., Plana, F. and Artiñano, B. (1998). Seasonal evolution of suspended particles around a large coal-fired power station. *Atmos. Environ.* 32: 1963–1978.

Ristovski, Z., Morawska, L., Bofinger, N.D. and Hitchins, J. (1998). Submicrometer and supermicrometer particulate emission from spark ignition vehicles. *Environ. Sci. Technol.* 32: 3845–3852.

Schwartz, J., Dockery, D.W. and Neas, L.M. (1996). Is daily mortality associated specifically with fine particles?" *J. Air Waste Manage. Assoc.* 46: 927–939.

Schwarz, J., Štefancová, L., Maenhaut, W., Smolík, J. and Ždímal, V. (2012). Mass and chemically speciated size distribution of Prague aerosol using an aerosol dryer--the influence of air mass origin. *Sci. Total Environ.* 437: 348–362.

Seinfeld, J.H. and Pandis, S.N. (2012). *Atmospheric Chemistry and Physics: From Air Pollution to Climate Change*. John Wiley & Sons, Hoboken, New Jersey, USA.

Smolík, J., Dohányosová, P. and Schwarz, J. (2008). Characterization of indoor and outdoor aerosols in a suburban area of prague. *Water Air Soil Pollut. Focus* 8: 35–47.

Smolík, J., Mašková, L., Zikova, N., Ondráčková, L. and Ondráček, J. (2013). Deposition of suspended fine particulate matter in a library. *Heritage Science* 1: 7.

Štefancová, L., Schwarz, J., Mäkelä, T., Hillamo, R. and Smolík, J. (2011). Comprehensive characterization of original 10-Stage and 7-Stage modified berner type impactors. *Aerosol Sci. Technol.* 45: 88–100.

Stelson, A.W. and Seinfeld, J.H. (1982). Relative humidity and temperature dependence of the ammonium nitrate dissociation constant. *Atmos. Environ.* 16: 983–992.

Talbot, N., Kubelova, L., Makes, O., Cusack., Ondracek, J., Vodička, P., Schwarz, J. and Zdimal, V. (2016). Outdoor and indoor aerosol size, number, mass and compositional dynamics at an urban background site during warm season. *Atmos. Environ.* 131: 171–184.

Tsai, J.H., Lin,J.H., Yao, H.C. and Chiang, H.L. (2012). Size distribution and water soluble ions of ambient particulate matter on episode and non-episode days in Southern Taiwan. *Aerosol Air Qual. Res.* 12: 263–274.

Vette, A.F., Rea, A.W., Lawless, P.A., Rodes, C.E., Evans, G., Highsmith, V.R. and Sheldon, L. (2001). Characterization of indoor-outdoor aerosol concentration relationships during the Fresno PM exposure studies. *Aerosol Sci. Technol.* 34: 118–126.

Vodička, P., Schwarz, J. and Ždímal, V. (2013). Analysis of one year's OC/EC data at a Prague suburban site with 2-h time resolution. *Atmos. Environ.* 77: 865–872.

Wallace, L. (1996). Indoor particles: A review. *J. Air Waste Manage. Assoc.* 46: 98–126.

Zhu, C.S., Cao, J.J., Shen, Z.X., Liu, S.X., Zhang, T., Zhao, Z.Z., Xu, H.M. and Zhang, E.K. (2012). Indoor and outdoor chemical components of $PM_{2.5}$ in the rural areas of northwestern China. *Aerosol Air Qual. Res.* 12: 1157–1165.

Zhu, Y., Hinds, W.C., Krudysz, M., Kuhn, T., Froines, J. and Sioutas, C. (2005). Penetration of freeway ultrafine particles into indoor environments. *J. Aerosol Sci.* 36: 303–322.

Zíková, N. and Ždímal, V. (2013). Long-term measurement of aerosol number size distributions at rural background station Košetice. *Aerosol Air Qual. Res.* 13: 1464–1474.

Received for review, September 2, 2016
Revised, December 19, 2016
Accepted, December 27, 2016